

## REGULATIONS OF THE FORMATION OF PROTECTIVE POTENTIAL OF UNDERGROUND STEEL PIPELINES UNDER CONDITIONS OF HETEROGENEOUS ENVIRONMENT

O.O. Aziukovskiy\*, Yu.A. Papaika\*\*, V.N. Gorev\*\*\*, N.V. Babenko\*\*\*\*

Dnipro University of Technology,  
Dmytro Yavornytskyi Ave., 19, Dnipro, 49005, Ukraine.  
E-mail: [papaika.yu.a@nmu.one](mailto:papaika.yu.a@nmu.one).

*In the work, the modeling of the distribution of the protective potential of electrochemical protection stations is performed by revealed functional dependencies. The initial conditions are adopted for a typical assortment of rolled metal used for underground gas supply. At the initial stage of modeling, the stochastic nature of the change in soil parameters is not taken into account. The distribution of the protective potential of the underground pipeline as a function of two variables (time and distance) showed the mutual influence of neighboring stations on the formation of protective zone. New dependences of the operating parameters of the electrotechnical complex of electrochemical protection on the set of variables characterizing the power source, the physical dimensions of pipeline and the alternative arrangement of active cathodic protection stations (CPS) were obtained. Experimental studies of the modes of electrochemical protection stations at the objects of the gas transportation system of Ukraine confirmed the adequacy of the proposed analytical models. References 16, Figures 3.*

**Keywords:** underground pipelines, electrochemical corrosion, cathodic protection, protection anode, electrochemical protection complex, protective potential.

**Introduction.** The gas transportation system of Ukraine is a complex of the underground and surface communications, which are combined into a single strategic system of energy supply for industrial facilities and housing stock. The problem related to the protection of underground pipelines against electrochemical corrosion is complex, multifaceted and not finally resolved today.

The variety of laying conditions, physical dimensions of the pipeline, the presence of nearby engineering communications and routes of electrified transport do not allow the development of a universal methodology for selecting the parameters of protective electrical engineering complexes for successful long-term protection of metal structures [1]. In the process of developing a comprehensive strategy for the protection of the high- and medium-pressure gas pipelines, the special models for determining the number and power of cathodic stations and special topology in their location were proposed. The difficulties of realizing the stable value of protective potential along the entire length of the pipeline led to the need for the analytical and physical modeling of functional dependence  $U(z, t)$  (where  $U$  is the protective potential;  $z$  is the distance in meters;  $t$  is the time) taking into account all possible combinations of initial conditions and available modern electrical equipment [2, 3].

*The purpose of this work* is to determine the analytical models of changes in the level of protective potential of electrochemical protection stations, taking into account various technical configurations of the metal structure itself and modes of controlled inverters to implement the successful protection with maximum energy efficiency [4-6].

**Analytical functional dependence of protective potential.** Let us consider the empty infinite underground steel cylindrical pipe with outer radius  $r=30$  mm and wall thickness  $h_p=4$  mm, the center of which is located at depth  $H=1.5$  cm. Let the pipe be placed in uniform soil with conductivity  $\sigma_s=2 \cdot 10^{-2} \Omega^{-1} \cdot \text{m}^{-1}$ . Let us consider the monochromatic case when the system parameters are changed with frequency  $f=25$  kHz. The insulation is considered to be very good with resistivity  $R_i=10^6 \Omega \cdot \text{m}$ .

The steel and soil damping factor are calculated as follows [1, 7]:

$$\gamma_{st} = \sqrt{\frac{\omega \mu_0 \mu_{st} \sigma_{st}}{2}}, \quad \gamma_s = \sqrt{\frac{\omega \mu_0 \sigma_s}{2}}, \quad (1)$$

where  $\mu_0=4\pi \cdot 10^{-7}$  H/m is the magnetic constant;  $\omega=2\pi f$  is the angular frequency;  $\mu_{st}=200$  is the magnetic conductivity of steel;  $\sigma_{st}$  is the steel conductivity,  $\sigma_{st}=1/\rho_{st}$ ;  $\rho_{st}=1.3 \cdot 10^{-7} \Omega \cdot \text{m}$  is the steel resistivity.

---

© Aziukovskiy O.O., Papaika Yu.A., Gorev V.N., Babenko N.V., 2024

ORCID: \* <https://orcid.org/0000-0003-1901-4333>; \*\* <https://orcid.org/0000-0001-6953-1705>;

\*\*\* <https://orcid.org/0000-0002-9528-9497>; \*\*\*\* <https://orcid.org/0000-0003-2309-0291>

The pipe impedance  $Z$ , transient resistance  $R_t$  and propagation constant  $\alpha$  are calculated as in [8]:

$$Z = \frac{\omega\mu_0}{8} + i \frac{\omega\mu_0}{2\pi} \ln\left(\frac{1,3}{\gamma_s r}\right) + \frac{(1-i)\gamma_{st}}{2\pi r \sigma_{st}} \cot\left((1-i)\gamma_{st} h_p\right), \quad R_t = R_i + \frac{1}{\pi\sigma_s} \ln\left(\frac{1,12}{\gamma_s \sqrt{rH}}\right), \quad \alpha = \sqrt{\frac{Z}{R_t}}, \quad (2)$$

where  $i = \sqrt{-1}$  is the imaginary unit; it should be noted that  $[Z]=\Omega/\text{m}$ ,  $[R_t]=\Omega \cdot \text{m}$  and  $[\alpha]=\text{m}^{-1}$ .

As shown in [1], the complex amplitudes of the potential along the pipe  $V(z)$  and the current along the pipe  $I(z)$  obey the following equations:

$$\frac{dV(z)}{dz} = -ZI(z), \quad V(z) = -R_t \frac{dI(z)}{dz} + \varphi(z), \quad (3)$$

where  $\varphi(z)$  is the potential of external electric field and  $z$  is the coordinate along the pipe.

As shown in [9] by (3), the function  $V(z)$  satisfies the following differential equation:

$$\frac{d^2V(z)}{dz^2} - \alpha^2 V(z) = -\alpha^2 \varphi(z). \quad (4)$$

In this paper we consider the case without external electric field and the corrosion protection stations are connected to the pipe. Let the station produces the potential difference between the point on steel pipe surface and the point located at the same depth as the center of the pipe at distance  $y$  from the center of the pipe. According to [10], the potential difference between these points can be expressed as

$$\Delta V(z) = -R_{st-s} \cdot \frac{dI(z)}{dz}, \quad R_{st-s} = R_i + \frac{1}{2\pi\sigma_s} \ln\left(\frac{y\sqrt{y^2 + 4H^2}}{2rH}\right). \quad (5)$$

Here and in the following, we consider the fact that  $\varphi(z)=0$  in the problem under consideration. One can conclude from (5) and (3) that

$$V(z) = \frac{R_t}{R_{st-s}} \Delta V(z). \quad (6)$$

First of all, let us assume that one station is located at coordinate  $z=0$  and produces the corresponding potential difference

$$\Delta U(z=0, t) = V_a \cos(\omega t). \quad (7)$$

Then

$$\Delta V(0) = V_a, \quad V(0) = \frac{R_t}{R_{st-s}} V_a. \quad (8)$$

Since  $\varphi(z)=0$  in the problem under consideration, equation (4) has the solution

$$V(z) = Ae^{\alpha z} + Be^{-\alpha z}, \quad (9)$$

where constants  $A, B$  can be chosen by (7) and taking into account the fact that the potential obviously cannot increase exponentially if  $z \rightarrow \pm\infty$ . So, the solution is expressed as

$$V(z) = \begin{cases} \frac{R_t}{R_{st-s}} V_a e^{\alpha z}, & z < 0 \\ \frac{R_t}{R_{st-s}} V_a e^{-\alpha z}, & z \geq 0 \end{cases}. \quad (10)$$

This leads to the following expression for the potential as a function of coordinate and time

$$U(z, t) = \text{Re}\left(V(z) e^{i\omega t}\right) = \begin{cases} \frac{R_t}{R_{st-s}} V_a e^{\alpha_1 z} \cos(\omega t + \alpha_2 z), & z < 0 \\ \frac{R_t}{R_{st-s}} V_a e^{-\alpha_1 z} \cos(\omega t - \alpha_2 z), & z \geq 0 \end{cases}, \quad (11)$$

where  $\alpha_1 = \text{Re}(\alpha)$ ,  $\alpha_2 = \text{Im}(\alpha)$ ; it should be noted that  $\alpha_1 > 0$ ,  $\alpha_2 > 0$ .

So, in the case of single station, the potential amplitude decreases exponentially, and the coordinate-dependent phase shift takes place [11].

Further let us consider two stations, one of them is placed at coordinate  $z=0$ , the other is located at  $z=L$ . Then the corresponding potential differences are

$$\Delta U(z=0, t) = V_{a1} \cos(\omega t + \varphi_1), \quad \Delta U(z=L, t) = V_{a2} \cos(\omega t + \varphi_2). \quad (12)$$

It also should be noted that in the general case the distances  $y_1, y_2$  and corresponding parameters  $R_{st-s1}$  and  $R_{st-s2}$  can not coincide. Thus

$$\Delta V(0) = V_a e^{i\varphi_1}, V(0) = \frac{R_t}{R_{st-s1}} V_a e^{i\varphi_1}, \Delta V(L) = V_a e^{i\varphi_2}, V(L) = \frac{R_t}{R_{st-s2}} V_a e^{i\varphi_2}. \quad (13)$$

We require the potential to be continuous, and the potential obviously cannot increase exponentially if  $z \rightarrow \pm\infty$ , so we seek the complex amplitude of the potential in the form

$$V(z) = \begin{cases} A e^{\alpha z}, & z < 0 \\ B e^{\alpha z} + C e^{-\alpha z}, & z \in [0, L], \\ D e^{-\alpha z}, & z > L \end{cases} \quad (14)$$

where in view of (13)

$$A = B + C, B e^{\alpha L} + C e^{-\alpha L} = D e^{-\alpha L}, A = \frac{R_t}{R_{st-s1}} V_a e^{i\varphi_1}, D e^{-\alpha L} = \frac{R_t}{R_{st-s2}} V_a e^{i\varphi_2}. \quad (15)$$

In fact (15) is a system of the equations linear in  $A, B, C$  and  $D$ . Its solution is

$$A = \frac{R_t}{R_{st-s1}} V_a e^{i\varphi_1}, B = \frac{R_t}{e^{\alpha L} - e^{-\alpha L}} \left( \frac{V_{a2}}{R_{st-s2}} e^{i\varphi_2} - \frac{V_{a1}}{R_{st-s1}} e^{i\varphi_1} e^{-\alpha L} \right), \quad (16)$$

$$C = \frac{R_t}{e^{\alpha L} - e^{-\alpha L}} \left( \frac{V_{a1}}{R_{st-s1}} e^{i\varphi_1} e^{\alpha L} - \frac{V_{a2}}{R_{st-s2}} e^{i\varphi_2} \right), D = \frac{R_t}{R_{st-s2}} V_a e^{i\varphi_2} e^{\alpha L}.$$

In view of (14) and (16), one can obtain the following expression:

$$V(z) = \begin{cases} \frac{R_t}{R_{st-s1}} V_{a1} e^{\alpha z} e^{i\varphi_1}, & z < 0 \\ V_{a1} \frac{R_t}{R_{st-s1}} \frac{\sinh(\alpha L - \alpha z)}{\sinh(\alpha L)} e^{i\varphi_1} + V_{a2} \frac{R_t}{R_{st-s2}} \frac{\sinh(\alpha z)}{\sinh(\alpha L)} e^{i\varphi_2}, & z \in [0, L], \\ \frac{R_t}{R_{st-s2}} V_{a2} e^{\alpha L} e^{-\alpha z} e^{i\varphi_2}, & z > L \end{cases} \quad (17)$$

whence

$$U(z, t) = \operatorname{Re}(V(z) e^{i\omega t}) = \begin{cases} U_1(z, t), & z < 0 \\ U_2(z, t), & z \in [0, L], \\ U_3(z, t), & z > L \end{cases} \quad (18)$$

where  $U_1(z, t) = \frac{R_t}{R_{st-s1}} V_{a1} e^{\alpha_1 z} \cos(\omega t + \alpha_2 z + \varphi_1)$ ,  $U_3(z, t) = \frac{R_t}{R_{st-s2}} V_{a2} e^{\alpha_1(L-z)} \cos(\omega t + \alpha_2(L-z) + \varphi_2)$ . (19)

The expression for  $U_2(z, t)$  is more complicated. Let us derive it. First of all, obviously

$$\sinh x = \frac{e^x - e^{-x}}{2} = \frac{e^{x_1 + ix_2} - e^{-x_1 - ix_2}}{2} = \sinh x_1 \cos x_2 + i \cosh x_1 \sin x_2, \quad x_1 = \operatorname{Re} x, \quad x_2 = \operatorname{Im} x, \quad (20)$$

whence

$$|\sinh x| = \sqrt{\sinh^2 x_1 \cos^2 x_2 + \cosh^2 x_1 \sin^2 x_2} = \sqrt{\frac{\cosh(2x_1) - \cos(2x_2)}{2}}, \quad (21)$$

and

$$\arg(\sinh x) = \operatorname{atan}(\cosh x_1 \sin x_2, \sinh x_1 \cos x_2), \quad (22)$$

where  $\operatorname{atan}$  is the so-called two-argument arctangent:

$$\operatorname{atan}(x_2, x_1) = \begin{cases} \arctan(x_2/x_1), & x_1 > 0 \\ \pi + \arctan(x_2/x_1), & x_1 < 0, x_2 \geq 0 \\ -\pi + \arctan(x_2/x_1), & x_1 < 0, x_2 < 0 \\ \pi/2, & x_1 = 0, x_2 > 0 \\ -\pi/2, & x_1 = 0, x_2 < 0 \\ \text{undefined}, & x_1 = x_2 = 0 \end{cases}. \quad (23)$$

From expressions (21), (22), (17) and (18), one can obtain the following expression for  $U_2(z, t)$ :

$$U_2(z, t) = V_{a1} \frac{R_t}{R_{st-s1}} \frac{h(L-z)}{h(L)} \cos(\omega t + g(L-z) - g(L) + \varphi_1) + \\ + V_{a2} \frac{R_t}{R_{st-s2}} \frac{h(z)}{h(L)} \cos(\omega t + g(z) - g(L) + \varphi_2), \quad (24)$$

where

$$h(z) = \sqrt{\cosh(2\alpha_1 z) - \cos(2\alpha_2 z)}, \quad g(z) = \text{atan}[\cosh(\alpha_1 z) \sin(\alpha_2 z), \sinh(\alpha_1 z) \cos(\alpha_2 z)]. \quad (25)$$

It should be underlined that function  $U(z, t)$  is essentially different when the stations have the same or opposite phases (see Figs. 1 and 2). The graphs, shown in Fig. 1 and Fig. 2 for  $\varphi_1 = \varphi_2 = 0$  and  $\varphi_1 = 0, \varphi_2 = \pi$ , respectively, are built for the following values:  $V_{a1} = V_{a2} = 3$  V,  $y_1 = y_2 = 0.1$  m,  $L = 3$  km.

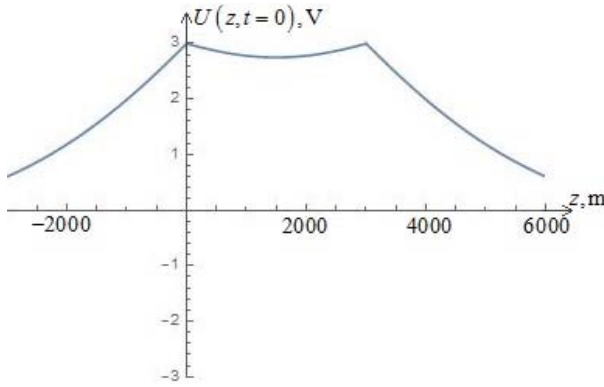


Fig. 1

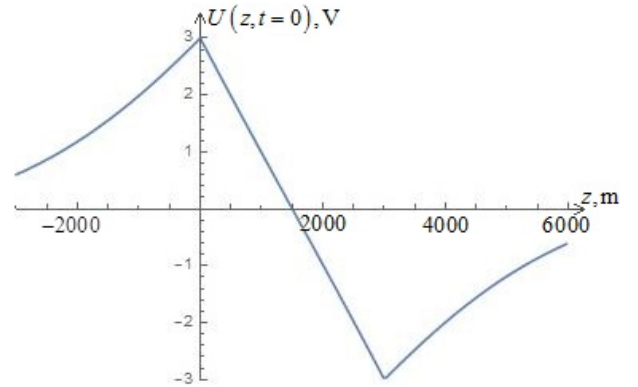


Fig. 2

Let us consider the case with  $V_{a1} = V_{a2} = V_a = 3$  V,  $y_1 = y_2 = y = 0.1$  m, and  $\varphi_1 = \varphi_2 = 0$ , parameter  $R_{st-s}$  is calculated on the basis of (5). Then function  $U_2(z, t)$  has the form [12, 13]

$$U_2(z, t) = \frac{V_a}{h(L)} \frac{R_t}{R_{st-s}} \left( h(L-z) \cos(\omega t + g(L-z) - g(L)) + h(z) \cos(\omega t + g(z) - g(L)) \right). \quad (26)$$

Let us find the absolute maximal deviation of function  $U_2(z, t)$  from the values

$$U_2(z=0, t) = U_2(z=L, t) = V_a \frac{R_t}{R_{st-s}} \cos(\omega t). \quad (27)$$

Let us rewrite (26) as

$$U_2(z, t) = \frac{V_a}{h(L)} \frac{R_t}{R_{st-s}} \left\{ \left[ h(L-z) \cos(g(L-z)) + h(z) \cos(g(z)) \right] \cdot \cos(\omega t - g(L)) - \right. \\ \left. - \left[ h(L-z) \sin(g(L-z)) + h(z) \sin(g(z)) \right] \cdot \sin(\omega t - g(L)) \right\}. \quad (28)$$

Let us denote

$$a(z) = h(L-z) \cos(g(L-z)) + h(z) \cos(g(z)), \quad b(z) = h(L-z) \sin(g(L-z)) + h(z) \sin(g(z)). \quad (29)$$

Then (28) can be rewritten as

$$U_2(z, t) = \frac{V_a}{h(L)} \frac{R_t}{R_{st-s}} \left[ a(z) \cdot \cos(\omega t - g(L)) - b(z) \cdot \sin(\omega t - g(L)) \right] = \\ = \frac{V_a}{h(L)} \frac{R_t}{R_{st-s}} \sqrt{a^2(z) + b^2(z)} \left[ \frac{a(z)}{\sqrt{a^2(z) + b^2(z)}} \cdot \cos(\omega t - g(L)) - \frac{b(z)}{\sqrt{a^2(z) + b^2(z)}} \cdot \sin(\omega t - g(L)) \right]. \quad (30)$$

The function  $\psi(z)$  exists such that according to [14]

$$\cos(\psi(z)) = \frac{a(z)}{\sqrt{a^2(z) + b^2(z)}}, \quad \sin(\psi(z)) = \frac{b(z)}{\sqrt{a^2(z) + b^2(z)}}, \quad \psi(z) = \text{atan}(b(z), a(z)), \quad (31)$$

therefore

$$U_2(z, t) = \frac{V_a}{h(L)} \frac{R_t}{R_{st-s}} \sqrt{a^2(z) + b^2(z)} \cos(\omega t - g(L) + \psi(z)) = V_a \frac{R_t}{R_{st-s}} A(z) \cos(\omega t + B(z)), \quad (32)$$

where

$$A(z) = \frac{\sqrt{a^2(z) + b^2(z)}}{h(L)}, \quad B(z) = \psi(z) - g(L). \quad (33)$$

Thus we have

$$\begin{aligned} \left| U_2(z, t) - V_a \frac{R_t}{R_{st-s}} \cos(\omega t) \right| &= V_a \frac{R_t}{R_{st-s}} \left| A(z) \cos(\omega t + B(z)) - \cos(\omega t) \right| = \\ &= V_a \frac{R_t}{R_{st-s}} \left| \left[ A(z) \cos(B(z)) - 1 \right] \cos(\omega t) - A(z) \sin(B(z)) \sin(\omega t) \right| = \\ &= V_a \frac{R_t}{R_{st-s}} \kappa(z) \left| \cos(\omega t + \theta(z)) \right|, \end{aligned} \quad (34)$$

where

$$\begin{aligned} \kappa(z) &= \sqrt{\left[ A(z) \cos(B(z)) - 1 \right]^2 + \left[ A(z) \sin(B(z)) \right]^2} = \sqrt{A^2(z) - 2A(z) \cos(B(z)) + 1}, \\ \theta(z) &= \operatorname{atan} \left( \frac{A(z) \sin(B(z))}{\kappa(z)}, \frac{A(z) \cos(B(z)) - 1}{\kappa(z)} \right). \end{aligned} \quad (35)$$

Hence

$$\max_{t,z} \left| U_2(z, t) - V_a \frac{R_t}{R_{st-s}} \cos(\omega t) \right| = V_a \frac{R_t}{R_{st-s}} \cdot \max_z \kappa(z), \quad z \in [0, L]. \quad (36)$$

One can conclude from (29), (31), (33) and (35) that

$$\kappa(z) = \kappa(L - z). \quad (37)$$

This implies

$$\kappa(z) = \frac{1}{2} (\kappa(z) + \kappa(L - z)) \quad (38)$$

and

$$\frac{d\kappa(z)}{dz} = \frac{1}{2} \left( \kappa'(z) + \kappa'(L - z) \frac{d(L - z)}{dz} \right) = \frac{1}{2} (\kappa'(z) - \kappa'(L - z)), \quad \kappa'(z) = \frac{d\kappa(z)}{dz}, \quad (39)$$

whence

$$\kappa'(L/2) = 0. \quad (40)$$

The computer plotting shows that function  $\kappa(z)$  has a single maximum at point  $z=L/2$  within the interval  $z \in [0, L]$  if, for example,  $L \leq 10$  km. The interesting question can arise: for what values of  $L$  the function  $\kappa(z)$  at  $z \in [0, L]$  has a single maximum at point  $z=L/2$ . However such question is not studied in this paper [15]. Thus,

$$\max_{t,z} \left| U_2(z, t) - V_a \frac{R_t}{R_{st-s}} \cos(\omega t) \right| = V_a \frac{R_t}{R_{st-s}} \cdot \kappa \left( \frac{L}{2} \right). \quad (41)$$

The simplified expression for  $\kappa(L/2)$  can be obtained. According to (29),

$$a \left( \frac{L}{2} \right) = 2h \left( \frac{L}{2} \right) \cos \left( g \left( \frac{L}{2} \right) \right), \quad b \left( \frac{L}{2} \right) = 2h \left( \frac{L}{2} \right) \sin \left( g \left( \frac{L}{2} \right) \right), \quad (42)$$

whence in accordance with (31) and (33),

$$A \left( \frac{L}{2} \right) = \frac{2h(L/2)}{h(L)}, \quad B \left( \frac{L}{2} \right) = \operatorname{atan} \left( 2h \left( \frac{L}{2} \right) \sin \left( g \left( \frac{L}{2} \right) \right), 2h \left( \frac{L}{2} \right) \cos \left( g \left( \frac{L}{2} \right) \right) \right) - g(L) = g \left( \frac{L}{2} \right) - g(L). \quad (43)$$

Here the definition (23) and the condition that  $h(L/2) > 0$  are used. Then in view of (41) and (35) we have

$$\begin{aligned} & \max_{t,z} |U_2(z,t) - U_2(z=0,t)| = \max_{t,z} |U_2(z,t) - U_2(z=L,t)| = \\ & = V_a \frac{R_t}{R_{st-s}} \cdot \sqrt{\frac{4h^2(L/2)}{h^2(L)} - 4 \frac{h(L/2)}{h(L)} \cos\left(g\left(\frac{L}{2}\right) - g(L)\right) + 1} = F(L), \end{aligned} \quad (44)$$

where functions  $h(z)$  and  $g(z)$  are determined by (25). For considered parameters [16], equation (44) is applicable, for example, when  $L \leq 10$  km. The function  $F(L)$  for  $V_{a1}=V_{a2}=V_a=3$  V,  $y_1=y_2=y=0.1$  m, and  $\varphi_1=\varphi_2=0$  is plotted in Fig. 3.

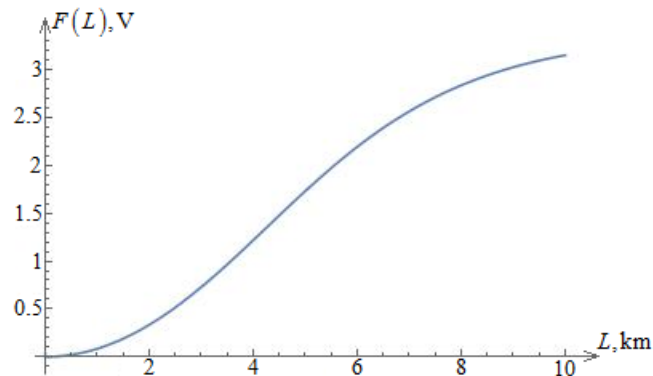


Fig. 3

## Conclusion

1. The analysis of conditions for effective protection against electrochemical corrosion of the electrotechnical complex “underground pipeline – a group of cathodic protection stations” made it possible to obtain their unique following features. The heterogeneity of soil has an effect on the gradient of the protective potential of cathodic stations, the point inhomogeneities in the form of crossings of railways, highways, cable underground lines of power transmission and the stochastic nature of the mutual influence of specified factors on the resulting type of electromagnetic field from a group of cathodic stations.

2. Taking into account the mandatory compliance with strict requirements for the distribution of protective potential along the entire length of pipeline, this article presents the mathematical modeling of protective potential distribution under reasonable initial conditions and assumptions. The assumption on the homogeneous nature of soil and the constant resistance of insulation made it possible to obtain the limiting values of potential variation depending on the physical parameters of the pipeline, time and distance.

3. The use of the proposed analytical and graphical dependences for various operating conditions of cathodic stations on longitudinal coordinate allows to improve significantly the quality of the formation of protective potential function. This characterizes the obtained scientific results in relation to the evaluation of energy-efficient modes of underground pipeline protection against electrochemical corrosion.

4. The results of modeling of external electric field along the underground pipeline revealed the possible limits in protective potential variation depending on the initial voltage phase of neighboring stations. The variable nature of the function of protective potential at the distance of 0–3000 m determines the need and importance to take into account the complex inhomogeneities for the development of universal method for selecting the technical parameters of electrotechnical protection complex and optimal operation mode.

1. Strizhevskij I.V., Dmitriev V.I. Theory and calculation of the influence of an electrified railway on underground metal structures. Moskva: Izdatelstvo stroitelnoi literatury, 1967. 249 p. (Rus).

2. Kulikov P., Aziukovskiy O., Vahonova O., Bondar O., Akimova L., Akimov O. Postwar Economy of Ukraine: Innovation and Investment Development Project. *Economic Affairs*. 2022. Vol. 67. No 5. Pp. 943–959. DOI: <https://doi.org/10.46852/0424-2513.5.2022.30>.

3. Montanari G.C., Fabiani D., Morshuis P., Dissado L. Why residual life estimation and maintenance strategies for electrical insulation systems have to rely upon condition monitoring. *IEEE Transaction on Dielectrics and Electrical Insulation*. 2016. Vol. 23(3). Pp. 1375–1385. DOI: <https://doi.org/10.1109/TDEI.2015.005613>.

4. Kucheriava I.M. Potential means for mitigation of magnetic field generated by underground power cables in polyethylene pipes made of composite magnetic material. *Tekhnichna Elektrodynamika*. 2023. No 3. Pp. 3–12. DOI: <https://doi.org/10.15407/techned2023.03.003> (Ukr).

5. Aziukovskiy A. The electrochemical cathodic protection stations of underground metal pipelines in uncoordinated operation mode. CRC Press. Balkema is an imprint of the Taylor & Francis Group, an informa business. London, UK, 2013. Pp. 47–55.

6. Shcherba M.A. Multi-physical processes during electric field disturbance in solid dielectric near water micro-inclusions connected by conductive channels. IEEE 2<sup>nd</sup> International Conference on *Intelligent Energy and Power Systems (IEPS)*. Kyiv, Ukraine, June 7-11, 2016. Pp. 1–5. DOI: <https://doi.org/10.1109/IEPS.2016.7521842>.
7. Shcherba M., Shcherba A., Peretyatko Y. Mathematical Modeling of Electric Current Distribution in Water Trees Branches in XLPE Power Cables Insulation. Proc. IEEE 7<sup>th</sup> International Conference on *Energy Smart Systems (ESS 2020)*. Kyiv, Ukraine, May 12-14, 2020. Pp. 353–356. DOI: <https://doi.org/10.1109/ESS50319.2020.9160293>.
8. Kyrylenko O.V., Shcherba A.A., Kucheriava I.M. Intellectual technologies for monitoring of technical state of up-to-date high-voltage cable power lines. *Tekhnichna Elektrodynamika*. 2021. No 6. Pp. 29–40. DOI: <https://doi.org/10.15407/techned2021.06.029> (Ukr).
9. Shcherba A.A., Podoltsev O.D., Kucheriava I.M. The study of magnetic field of power cables in polyethylene pipes with magnetic properties. *Tekhnichna Elektrodynamika*. 2020. No 3. Pp. 15–21. DOI: <https://doi.org/10.15407/techned2020.03.015> (Ukr).
10. Artemenko M.Yu., Batrak L.M., Polishchuk S.Y. Current Filtering in Three-Phase Three-Wire Power System at Asymmetric Sinusoidal Voltages. Proceedings of the IEEE 38<sup>th</sup> International Conference on *Electronics and Nanotechnology (ELNANO)*. Kyiv, Ukraine, 24–26 April 2018. Pp. 611–616. DOI: <https://doi.org/10.1109/ELNANO.2018.8477580>.
11. Franchuk V.P., Ziborov K.A., Krivda V.V., Fedoriachenko S.O. Influence of thermophysical processes on the friction properties of wheel – rail pair in the contact area. *Naukovyi Visnyk Natsionalnoho Hirnychoho Universytetu*. 2018. No 2. Pp. 46–52. DOI: <https://doi.org/10.29202/nvngu/2018-2/7>.
12. Beshta O., Beshta D., Balakhontsev O., Khudoliy S. Energy saving approaches for mine drainage systems. *Technical and Geoinformational Systems in Mining: School of Underground Mining*. London: CRC Press, 2011. Pp. 29–32.
13. Pivnyak G., Beshta A., Balakhontsev A. Efficiency of water supply regulation principles. *New Techniques and Technologies in Mining*. London: CRC Press, 2011. Pp. 1-8. DOI: <https://doi.org/10.1201/b113292>.
14. Pivnyak G., Zhezhelhenko I., Papaika Y. Estimating economic equivalent of reactive power in the systems of enterprise power supply. *Naukovyi Visnyk Natsionalnoho Hirnychoho Universytetu*. 2016. No 5. Pp. 62–66.
15. Pivnyak G., Rogoza M., Papaika Y., Lysenko A. Traction and energy characteristics of nocontact electric mining locomotives with AC current thyristor converters. *Power Engineering, Control and Information Technologies in Geotechnical Systems*. London: CRC Press, 2015. 220 p. DOI: <https://doi.org/10.1201/b18475>.
16. Beshta A., Beshta A., Balakhontsev A., Khudoliy S. Performances of asynchronous motor within variable frequency drive with additional power source plugged via combined converter. IEEE 6<sup>th</sup> International Conference on *Energy Smart Systems (ESS)*. Kyiv, Ukraine, 17–19 April 2019. Pp. 156–160. DOI: <https://doi.org/10.1109/ESS.2019.8764192>.

УДК 621.314

## ЗАКОНОМІРНОСТІ ФОРМУВАННЯ ЗАХИСНОГО ПОТЕНЦІАЛУ ПІДЗЕМНИХ СТАЛЕВИХ ТРУБОПРОВОДІВ В УМОВАХ НЕОДНОРІДНОГО СЕРЕДОВИЩА

**О.О. Азюковський**, канд. техн. наук, **Ю.А. Папаїка**, докт. техн. наук, **В.М. Горєв**, канд. техн. наук, **М.В. Бабенко**  
 НТУ «Дніпровська політехніка»,  
 пр. Дмитра Яворницького, 19, Дніпро, 49005, Україна.  
 E-mail: [papaika.vu.a@nmu.one](mailto:papaika.vu.a@nmu.one).

У роботі виконано моделювання розподілу захисного потенціалу станцій електрохімічного захисту на основі отриманих функціональних залежностей. Початкові умови прийнято для типового сортаменту металопрокату, що застосовується для підземного газопостачання. На початковому етапі моделювання стохастичний характер зміння параметрів ґрунтів не враховано. Розподіл захисного потенціалу підземного трубопроводу в функції двох змінних (часу та дистанції) показав взаємний вплив сусідніх станцій на формування захисної зони. Отримано нові залежності режимних параметрів електротехнічного комплексу електрохімічного захисту від комплексу змінних, що характеризують джерело живлення, фізичні розміри трубопроводу та варіативне розташування активних катодних станцій. Експериментальні дослідження режимів станцій електрохімічного захисту на об'єктах газотранспортної системи України підтвердили адекватність запропонованих аналітичних моделей. Бібл. 16, рис. 3.

**Ключові слова:** підземні трубопроводи, електрохімічна корозія, катодний захист, захисний анод, комплекс електрохімічного захисту, захисний потенціал.

Надійшла 20.11.2023  
 Остаточний варіант 13.02.2024